

Control of Active Nematics with Passive Liquid Crystals

Pau Guillamat, Jordi Ignés-Mullol*, and Francesc Sagués

Department of Materials Science and Physical Chemistry, and Institute of Nanoscience and Nanotechnology, University of Barcelona, Barcelona, Catalonia, Spain

* Marti i Franquès 1, 08028 Barcelona, Catalonia, Spain. E-mail: jignes@ub.edu

Author contact information:

Pau Guillamat

Email: pauguillamat@gmail.com

Phone: +34 934039252

FAX: +34 934212131

Jordi Ignés-Mullol

Email: jignes@ub.edu

Phone: +34 934039290

FAX: +34 934212131

Francesc Sagués

Email: f.sagues@ub.edu

Phone: +34 934021242

FAX: +34 934212131

Control of Active Nematics with Passive Liquid Crystals

Motor-proteins are responsible for transport inside cells. Harnessing their activity is key towards developing new nano-technologies, or functional biomaterials. Cytoskeleton-like networks result from the self-assembly of subcellular autonomous units. Taming this biological activity bottom-up may thus require molecular level alterations compromising protein integrity. Taking a top-down perspective, here we prove that the seemingly chaotic flows of a tubulin-kinesin active gel can be forced to adopt well-defined spatial directions by tuning the anisotropic viscosity of a contacting Smectic-A liquid crystal. Different configurations of the active material are realized, when the thermotropic liquid crystal is either unforced or commanded by a magnetic field. The inherent instability of the extensile active fluid is thus spatially regularized, leading to organized flow patterns, endowed with characteristic length and time scales. Our finding paves the way for designing hybrid active/passive systems where ATP-driven dynamics can be externally conditioned.

Keywords: active matter; active nematic; focal conics, Smectic-A; magnetic-field alignment;

Introduction

Cytoskeleton reconstitutions are structured soft systems displaying characteristics of self-assembled colloidal dispersions, but, distinctively, they are active¹⁻¹¹. Under suitably constrained conditions, and with a steady supply of ATP, these new types of materials feature emergent modes of self-organization that arise from the collective behavior of individual biomolecules. Besides posing fascinating questions, related to the permanent and intrinsic non-equilibrium nature of these systems^{12, 13}, the fact that they constitute *in vitro* models for the intra-cellular milieu suggests a potential for the development of new responsive biomaterials. For instance, one could envision to externally commanding the preferred flow lines, deformation directions, or intrinsic entanglements of these active gels, although a successful strategy in this direction has yet to be demonstrated. The complexity and specificity of the involved components seems to preclude an *a priori*

process of protein engineering. It seems thus advisable to devise a control strategy with the potential of being exerted on any viable active gel. Actuating by means of either an electric or a magnetic field is unlikely, given the high ionic strength of these preparations, which screens electric responses, and the low magnetic susceptibilities that make them insensitive to modest magnetic forces. On the other hand, one could resort to the confinement of the active material in patterned microfluidic channels, which will determine the direction and time scales of its spontaneous active deformations. This procedure has the disadvantage of requiring complex biochemical functionalization of the inner surfaces to render the substrates biocompatible but, even if successful, this strategy will be neither versatile nor *in situ* reconfigurable. Here, we demonstrate a radically different approach by interfacing the aqueous active gel with a thermotropic liquid crystal that features the Nematic to Smectic-A (SmA) transition at a biocompatible temperature¹⁴. We take advantage of the fact that the Nematic phase can be easily aligned under a modest magnetic field, and of the fact that the SmA phase features a dramatic anisotropy in the shear viscosity. We employ these features to tame the seemingly chaotic flows of protein gels.

Experimental Section

Preparation of the Active Nematic

As a precursor of the active nematic, we prepare an active gel of tubulin microtubules (MT) crosslinked by clusters of the molecular motor kinesin following the protocols detailed elsewhere¹⁵. Briefly, the MT are polymerized from bovine brain tubulin (a gift from Z. Dogic's group in Brandeis University) with a typical length 1 – 2 μm . For fluorescence microscopy, a fraction of the tubulin (3 %) has been fluorescently labelled with Alexa-647. The motor protein kinesin-1 from *Drosophila Melanogaster* is expressed

in *E. Coli*, purified, and incubated in the presence of the protein streptavidin. This leads to the assembly of clusters that contain, on average, two of the biotinylated motor proteins. The MT are mixed with a solution containing the non-adsorbing polymer polyethylene glycol (PEG, 20kDa) and the kinesin clusters. PEG acts as a depleting agent, promoting the bundling of the MT into filaments, while the motor clusters act as cross-linkers of the gel. In the presence of Adenosine Triphosphate (ATP), kinesin promotes the sliding of MT bundles of opposite polarity, thus resulting in an extensile active gel. A PEG-based triblock copolymer surfactant (Pluronic F-127) is added to the protein mixture. This leads to the formation of a biocompatible interface when the liquid crystal and the aqueous medium are put into contact, and promotes the depletion of the active gel towards the soft interface, which leads to the formation of the quasi-two-dimensional active nematic when the filaments develop long-range orientational order.

Experimental Setup

The water/LC interface is prepared in a custom flow cell made using the commonly used transparent elastomer PDMS placed onto a glass plate coated with a hydrophilic and bio-inert polyacrylamide brush. The cylindrical cavity is filled with 50 μL octyl-cyanobiphenyl (8CB, Nematel) and 1 μL of the aqueous protein suspension is injected between the oil and the hydrophilic substrate, which is coated by the water phase. The system is heated to 35 $^{\circ}\text{C}$ to promote the transition of 8CB, which is in the SmA phase at room temperature, into the less viscous Nematic phase.

Temperature Control and Magnetic Field Application

Polarizing and fluorescence microscopy is carried out in a custom optomechanical setup built around a custom-made permanent magnet assembly that provides homogeneous planar magnetic field in a region much larger than the field of view, with a maximum

strength of 0.4 T. The magnet is a Halbach array of 25.4 mm commercial cubic magnets, custom designed and built as described elsewhere¹⁵. Samples are held inside a thermostatic oven build with Thorlabs SM1 tube components and tape heater, and controlled with a Thorlabs TC200 controller.

Observation and Characterization

Routine observation of the active nematic is performed by means of a conventional epifluorescence microscope, while laser-scanning confocal microscopy (both in fluorescence and reflection modes) is employed when sharper images are required.

Results and discussion

Formation of rotating mills in contact with Toroidal Focal Conic Domains

The chosen active material is based on the self-assembly of tubulin, from protein monomers all the way up to filamentary bundles of micron-sized stabilized microtubules^{6, 16}. The latter are cross-linked and sheared by clusters of ATP-fueled kinesin motors, which are directed towards the plus ends of the microtubules. Inter-filament sliding thus occurs in bundles containing microtubules of opposite polarity (Fig. 1A). This mixture self-assembles into an extensile active gel¹⁷⁻¹⁹, continuously rebuilt following bundle reconstitution, and permanently permeated by streaming flows. An alternative preparation, more suited to our purposes, consists in depleting this bulk material towards a biocompatible soft and flat interface, where filaments continuously fold and adopt textures typical of a two-dimensional nematic⁶. This active layer appears punctuated by a steady number of continuously renovated microtubule-void regions that configure semi-integer defect areas. Although we focus on flat interfaces, the latter can be also curved, giving rise to interesting defect accommodation dynamics, and occasionally to intriguing deformation modes of the, in this way prepared, active

vesicles²⁰. In our case, a layer of active gel is confined between a biocompatible hydrophilic rigid surface (bottom) and a (top) volume of the liquid crystal (LC) octylcyanobiphenyl (8CB), which features a Nematic/Smectic-A transition at around 33 °C, compatible with protein activity (Fig. 1B). The LC/water interface is stabilized with a polyethylene glycol (PEG)-based triblock copolymer surfactant.

To better appraise the role played by the contacting structured interface on the active material, the top passive liquid crystal is initially prepared in its Nematic phase. On average, the 8CB mesogen molecules lay parallel to the LC/water interface, due to the influence of the polymeric surfactant, and perpendicular to the LC/air interface far from the active layer. In the presence of isotropic oils, the contacting active nematic features the well-known disordered swirling motion, characterized by the formation and annihilation of defects²¹⁻²⁴, accompanying the spontaneous folding of the bundled microtubules. Although nematic 8CB is anisotropic, shear viscosities along different directions are of the same order of magnitude, and do not trigger any observable differences when compared with the contact with isotropic oils (Fig. 2, A-C). It is known, in the latter case, that there is a strong hydrodynamic coupling between the active and the passive fluids. Indeed, the oil viscosity influences both the density and velocity of proliferating defects in the active nematic. This gives us a clear indication that the contact of the active and passive structured materials is robust, persistent, and stable enough to foresee stronger effects when the order of the passive phase is further upgraded to the more anisotropic Smectic-A phase.

A temperature quench below 33.4 °C triggers the reversible transition of 8CB into the lamellar Smectic-A phase. This has a dramatic impact on the interfacial rheology and on the dynamics of the active nematic. Layers in the Smectic-A phase are perpendicular to the 8CB molecules, which remain parallel to the LC/water interface. Free-energy

minimization constraints, related to the boundary conditions at the interfaces, result in the formation of the so-called toroidal focal conics¹⁴. These are polydisperse circular domains that form a fractal tiling called Apollonius gasket²⁵. Inside the domains, radially-oriented mesogen molecules arrange concentrically at the oil/water interface (Fig. 2D). Flow perpendicular to the Smectic layers is severely hindered and, contrarily, is highly facilitated along them. As a result, the local interfacial shear stress experienced by the active material is markedly anisotropic. Stretching of the bundled filaments thus occurs preferably along circular trajectories centered with the focal conics, which organize the active nematic in confined rotating mills (Fig. 2E). Flows can be traced following the motion of the $+1/2$ comet-like defects, and become fully apparent from time-averaged snapshots of the active pattern (Fig. 2F). Dark spots, where filament occupancy is lowest, appear then in register with the center of large focal conics in the Smectic-A oil. Increasing the temperature, the Smectic phase of the passive liquid crystal melts down and, as expected, the rotating mills are completely and immediately dismantled, recovering the typical textures of the active nematic.

Filamentary bundles of the active material have an intrinsic maximum curvature that cannot be exceeded. As a consequence, only focal conics above a threshold diameter, which we have estimated at around $40\ \mu\text{m}$ in the experiment shown in Fig. 2, are able to coordinate the flow of the underlying active material. From a topological perspective, confined rotating filaments organize a topological singularity of charge $S=+1$, which corresponds to a full rotation around the domain center (Fig. 3). The semi-integer defects, which accompany rotating filaments, are permanently renovated, even their number may change to a small extent, assembling and disassembling continuously the core structure of the rotating mill. At all times, however, a balance is established such that the arithmetic sum of topological charges inside a single domain adds up to one

(Fig. 3). This collective precession is accompanied by a periodic modulation of the velocity of the active flows.

Reversible alignment of the active nematic with a magnetic field

A tighter control of the active flow is achieved by directly actuating on the contacting thermotropic liquid crystal. To this purpose, we take advantage of its large (positive) diamagnetic anisotropy that enables to align a macroscopic volume of the material with uniform magnetic fields of the order of a few kG, easily attainable with a permanent magnet array. By a slow temperature quench of 8CB from the nematic to the Smectic-A phase in presence of a 4 kG magnetic field parallel to the LC/water interface, we induce the formation of a layer of 8CB molecules uniformly aligned with the magnetic field. In this situation, the Smectic planes are oriented perpendicularly both to the interface and to the magnetic field (Fig. 4). It is well-known in the literature that this *bookshelf* geometry, robustly kept after removal of the magnetic field, results in a liquid that flows easily when sheared along the lamellar planes, but that responds as a solid to stresses exerted in the orthogonal direction¹⁴. Polarizing optical microscopy confirms the formation of this aligned smectic-A layer (Fig. 4A) that includes dislocations in the aligned lamellar planes, which propagate into the bulk of the material with the so-called parabolic focal conic domains. In contact with this interface, the turbulent active nematic experiences markedly anisotropic shear stresses, which result in a rapid rearrangement of the flow pattern that consists now in bands of uniform width, perpendicular to the magnetic field (Figs. 4 B-E). More precisely, stripes of densely stacked microtubules that appear bright in the fluorescence images, appear alternated with dark lanes of moving defects, along which antiparallel flow velocities are easily recognized, and clearly visualized using particle tracers. Negative defects are, in this situation, more difficult to localize, although the global topological requirement

mentioned earlier applies here to secure a zero total charge. As before, this organized structure is immediately and totally reset, to recover the standard well-mixed configuration of the active material, when reversing the temperature quench back to the Nematic phase of the thermotropic mesogen. Moreover, by previous transiting back and forth through the passive nematic 8CB phase, the orientation of the active pattern can be readily and reversibly in plane-rotated by redirecting the magnetic field at will (Fig. 4 D, E). The striped pattern defines a characteristic wavelength, which depends on the activity of the sample. This characteristic spatial periodicity is associated to a typical length scale in the active material, l_α , that has been predicted in theoretical studies to decrease with the square of the activity, and governs the decay of the flow vorticities and the director fields for unconfined active nematics²⁶. By approximating the activity parameter as $\alpha \sim \ln[ATP]$, we recover the predicted scaling of l_α (Fig. 5B).

Within stripes, bundles of microtubules are packed in parallel arrangements oblique to the lanes of moving defects (Fig. 6A, B). This microtubule disposition, although apparently motionless, is prone to suffer the bending instability intrinsic to any extensible active material^{27,28}. Following such instability, pairs of complementary half-integer defects are created and either they annihilate in pairs or incorporate into opposite preexisting lanes (Fig. 6C). Once defects escape from their birth areas, the striped regions are restored with minimal rearrangements. Such apparently vulnerable episodes of the active material extend coherently over regions of arbitrary extension but always commensurate with the stripe width, and occur periodically with a striking regularity. We conjecture that this kind of periodic “avalanches” arise from the intrinsic dynamics of the sheared microtubules, and provide a breakdown mechanism that the active

material has at its disposition to repeatedly release the extensile tensional stress accumulated in the stripes of the active material.

In summary, our work demonstrates that the disordered flow patterns of an active two-dimensional nematic can be controlled to follow preassigned directions. This is achieved by means of the anisotropic shear stress exerted at the interface by a thermotropic liquid crystal layer whose orientation can be externally commanded with a magnetic field. The ordered active material clearly reveals its characteristic time and length scales, which arise from non-equilibrium biochemical processes at the molecular level. The versatility, reversibility and robustness of such strategy should be considered as a proof of concept for the taming of active subcellular materials.

Acknowledgments

The authors are indebted to Z. Dogic and S. DeCamp (Brandeis University), and the Brandeis University MRSEC Biosynthesis facility for their assistance in the preparation of the active gel. We thank B. Hishamunda (Brandeis University), and M. Pons, A. LeRoux, and G. Iruela (Universitat de Barcelona) for their assistance in the expression of motor proteins. Funding has been provided by MINECO (project FIS 2013-41144P). P.G. acknowledges funding from Generalitat de Catalunya through a FI-DGR PhD Fellowship. Brandeis University MRSEC Biosynthesis facility is supported by NSF MRSEC DMR-1420382.

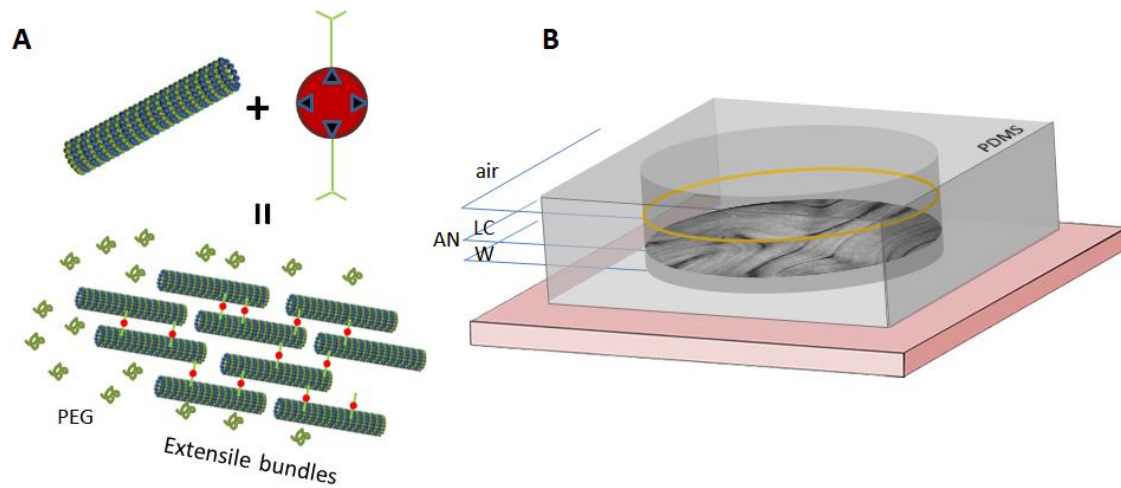


Figure 1. A: Tubulin microtubules are crosslinked into extensile bundles by clusters of kinesin motor proteins. Depletion interaction, originated by PEG present in the protein suspension, helps to condense the bundles. B: Flow cell used in the experiments. A 5 mm deep, 8 mm in diameter cylindrical cavity, custom made with the elastomer PDMS, is bound to a hydrophilic, biocompatible glass plate. The aqueous protein solution is in contact with the substrate, and a volume of LC is placed on top, defining the LC/water interface where the active nematic (AN) forms. The LC is open to the air at the top.

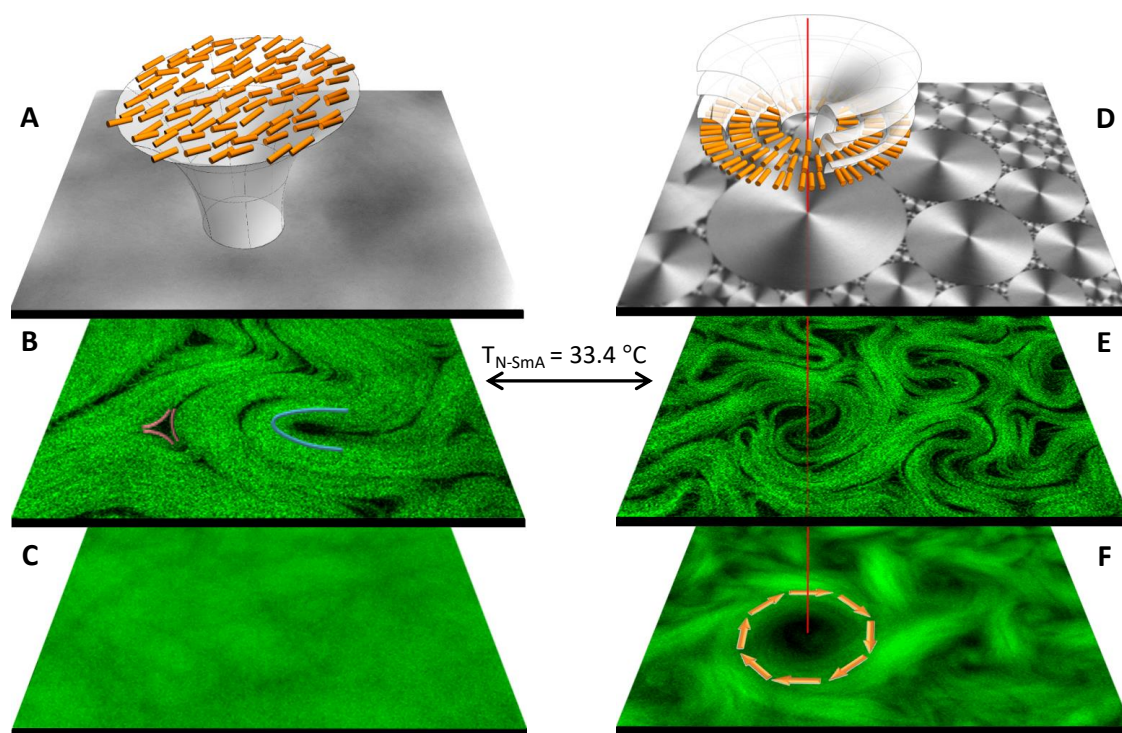


Figure 2. Self-assembly of the active layer in contact with the enforced liquid crystal. The active material is in contact either with the nematic (A-C) or the Smectic-A phase (D-F) of 8CB. Reversible transition between both states is observed at $33.4\text{ }^{\circ}\text{C}$. Confocal reflection micrographs of the interface reveal the featureless nematic 8CB phase, where molecules lay, on average, parallel to the oil/water interface, with short-range positional but long-range orientational correlations (A). Fluorescence confocal microscopy imaging of the active nematic depleted towards the nematic 8CB (B) reveals the characteristic semi-integer folds (highlighted in B) that dynamically form, annihilate, and move in a turbulent fashion, with no temporal coherence, as evidenced by the time average shown in (C). A temperature quench into the lamellar Smectic-A phase of 8CB results in the formation of the well-known toroidal focal conic domains, as revealed by confocal reflection imaging (D). Fluorescence confocal microscopy, both with fast (E) and time-averaged exposure (F) reveal the formation of rotating mills in the active nematic, in registry with the circular domains in 8CB. Micrographs are $244\text{ }\mu\text{m}$ wide.

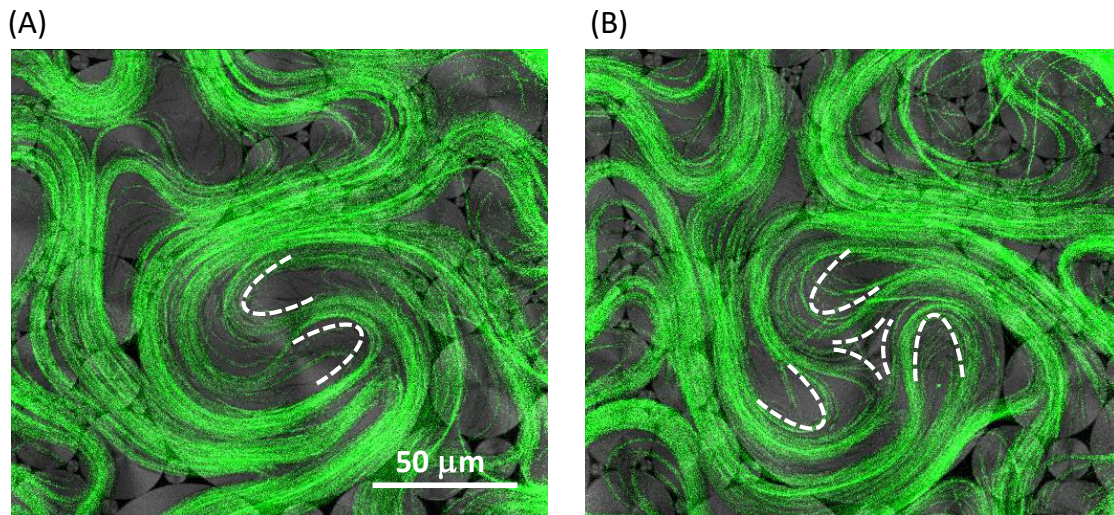


Figure 3. Fluorescence confocal micrograph showing two examples of the topological structure of a rotating mill of active nematic filaments preserves a constant topological charge $S=+1$ at all times. Defects in the rotating mill are highlighted with dashed lines and have a charge (A) $2 \times 1/2$, and (B) $3 \times 1/2 - 1/2$.

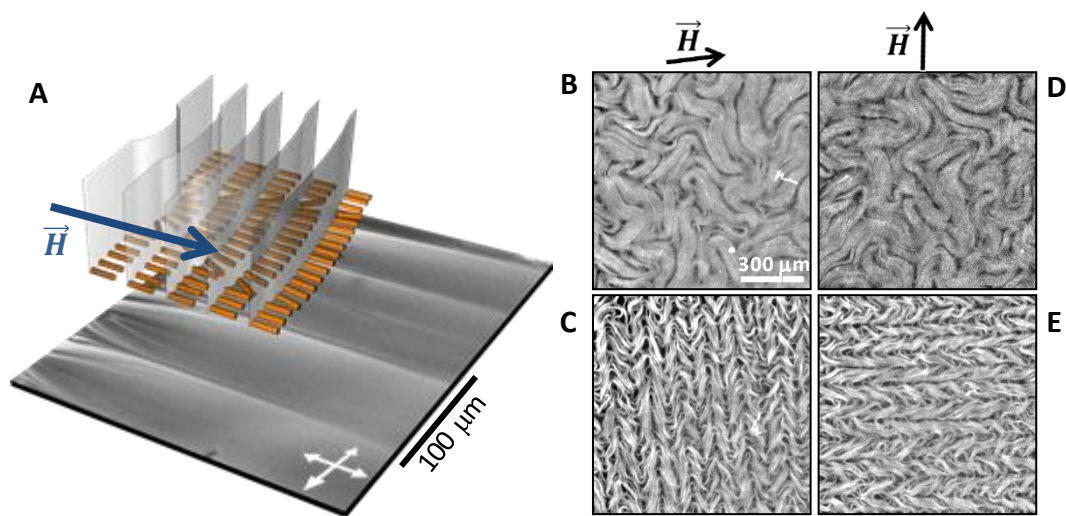


Figure 4. A: Polarized microscopy micrograph and sketch of the Smectic-A in the bookshelf configuration upon alignment with a magnetic field. B-D: Fluorescence micrographs of the active nematic interfaced with 8CB in different phases (Nematic in B, D; Smectic-A in C, E), in the presence of a magnetic field, as shown above each column.

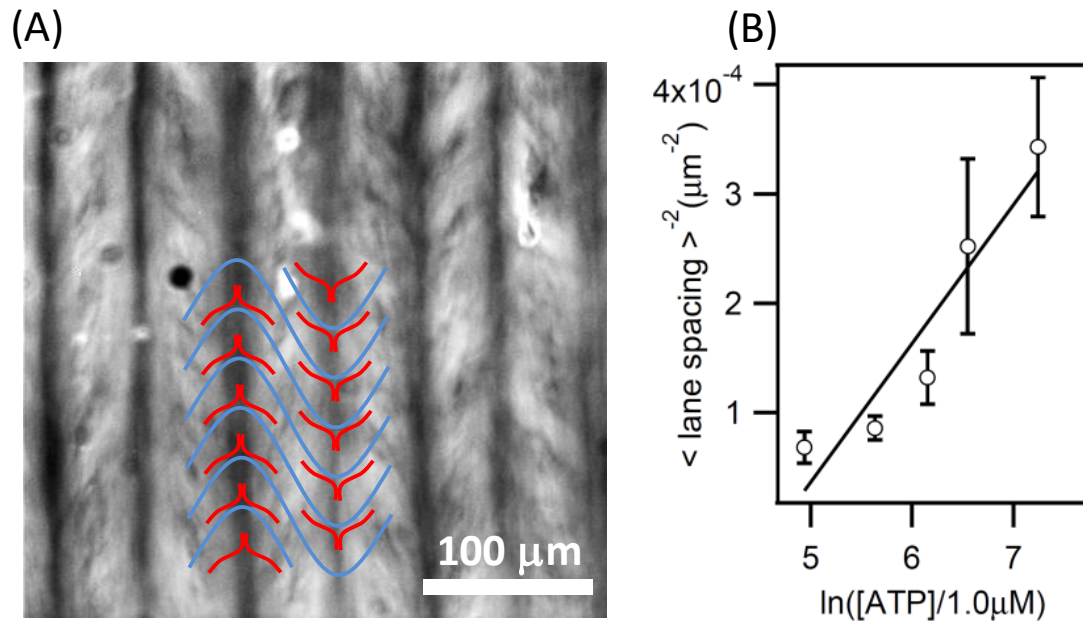


Figure 5. A: Fluorescence micrograph (long-time exposure) of the aligned active nematic. The lanes of alternated +1/2 (blue) and -1/2 (red) defects are shown. B: Dependence of lane spacing with activity.

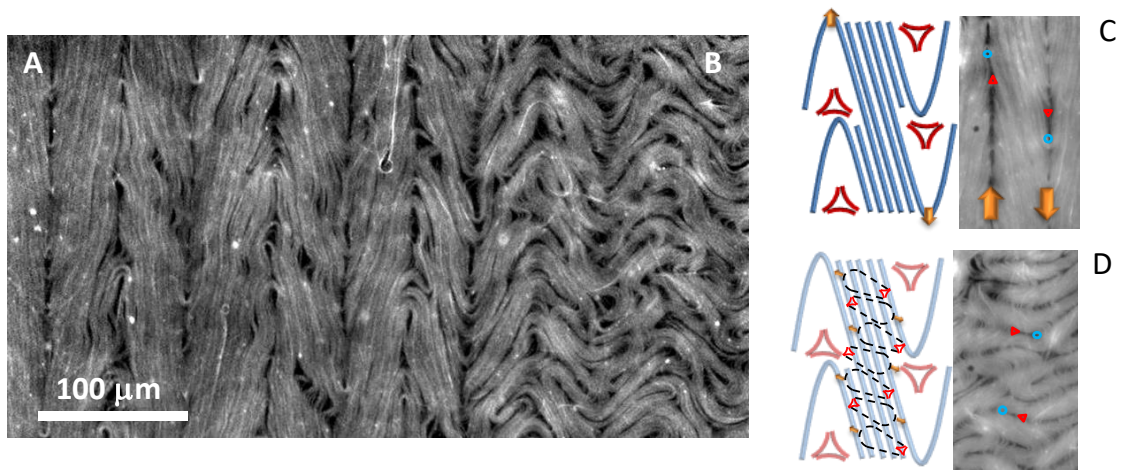


Figure 6. Fluorescence micrograph of the active nematic featuring the coexistence with a region with aligned stripes (A) and a region with the transversal instability (B). C, D: sketch of the configuration of the filaments, flow velocity, and defects in two adjacent flow lanes for the aligned and the unstable states, respectively.

1. DeCamp, S. J.; Redner, G. S.; Baskaran, A.; Hagan, M. F.; Dogic, Z., Orientational order of motile defects in active nematics. *Nat Mater* **2015**, 14, 1110-5.
2. Gao, T.; Blackwell, R.; Glaser, M. A.; Betterton, M. D.; Shelley, M. J., Multiscale polar theory of microtubule and motor-protein assemblies. *Phys Rev Lett* **2015**, 114, 048101.
3. Karsenti, E.; Nedelec, F.; Surrey, T., Modelling microtubule patterns. *Nat Cell Biol* **2006**, 8, 1204-11.
4. Kohler, S.; Schaller, V.; Bausch, A. R., Structure formation in active networks. *Nat Mater* **2011**, 10, 462-8.
5. Nedelec, F. J.; Surrey, T.; Maggs, A. C.; Leibler, S., Self-organization of microtubules and motors. *Nature* **1997**, 389, 305-8.
6. Sanchez, T.; Chen, D. T.; DeCamp, S. J.; Heymann, M.; Dogic, Z., Spontaneous motion in hierarchically assembled active matter. *Nature* **2012**, 491, 431-4.
7. Schaller, V.; Bausch, A. R., Topological defects and density fluctuations in collectively moving systems. *Proceedings of the National Academy of Sciences* **2013**, 110, 4488-4493.
8. Schaller, V.; Weber, C.; Semmrich, C.; Frey, E.; Bausch, A. R., Polar patterns of driven filaments. *Nature* **2010**, 467, 73-7.
9. Schaller, V.; Weber, C. A.; Hammerich, B.; Frey, E.; Bausch, A. R., Frozen steady states in active systems. *Proc Natl Acad Sci U S A* **2011**, 108, 19183-8.
10. Sumino, Y.; Nagai, K. H.; Shitaka, Y.; Tanaka, D.; Yoshikawa, K.; Chate, H.; Oiwa, K., Large-scale vortex lattice emerging from collectively moving microtubules. *Nature* **2012**, 483, 448-52.
11. Surrey, T.; Nedelec, F.; Leibler, S.; Karsenti, E., Physical properties determining self-organization of motors and microtubules. *Science* **2001**, 292, 1167-71.
12. Marchetti, M. C.; Joanny, J. F.; Ramaswamy, S.; Liverpool, T. B.; Prost, J.; Rao, M.; Simha, R. A., Hydrodynamics of soft active matter. *Reviews of Modern Physics* **2013**, 85, 1143-1189.
13. Ramaswamy, S., The Mechanics and Statistics of Active Matter. *Annual Review of Condensed Matter Physics* **2010**, 1, 323-345.
14. Oswald, P.; Pieranski, P., *Smectic and columnar liquid crystals : concepts and physical properties illustrated by experiments*. Taylor & Francis: Boca Raton, FL, 2006; p xx, 690 p.
15. Guillamat, P.; Ignés-Mullol, J.; Sagues, F., Control of active liquid crystals with a magnetic field. *Proc Natl Acad Sci U S A* **2016**, 113, 5498-502.

16. Henkin, G.; DeCamp, S. J.; Chen, D. T.; Sanchez, T.; Dogic, Z., Tunable dynamics of microtubule-based active isotropic gels. *Philos Trans A Math Phys Eng Sci* **2014**, 372.
17. Julicher, F.; Kruse, K.; Prost, J.; Joanny, J., Active behavior of the Cytoskeleton. *Physics Reports* **2007**, 449, 3-28.
18. Kruse, K.; Joanny, J. F.; Julicher, F.; Prost, J.; Sekimoto, K., Generic theory of active polar gels: a paradigm for cytoskeletal dynamics. *Eur Phys J E Soft Matter* **2005**, 16, 5-16.
19. Prost, J.; Jülicher, F.; Joanny, J. F., Active gel physics. *Nature Physics* **2015**, 11, 111-117.
20. Keber, F. C.; Loiseau, E.; Sanchez, T.; DeCamp, S. J.; Giomi, L.; Bowick, M. J.; Marchetti, M. C.; Dogic, Z.; Bausch, A. R., Topology and dynamics of active nematic vesicles. *Science* **2014**, 345, 1135-9.
21. Giomi, L.; Bowick, M. J.; Ma, X.; Marchetti, M. C., Defect annihilation and proliferation in active nematics. *Phys Rev Lett* **2013**, 110, 228101.
22. Shi, X. Q.; Ma, Y. Q., Topological structure dynamics revealing collective evolution in active nematics. *Nat Commun* **2013**, 4, 3013.
23. Thampi, S. P.; Golestanian, R.; Yeomans, J. M., Velocity correlations in an active nematic. *Phys Rev Lett* **2013**, 111, 118101.
24. Weber, C. A.; Bock, C.; Frey, E., Defect-mediated phase transitions in active soft matter. *Phys Rev Lett* **2014**, 112, 168301.
25. Meyer, C.; Le Cunff, L.; Belloul, M.; Foyart, G., Focal Conic Stacking in Smectic A Liquid Crystals: Smectic Flower and Apollonius Tiling. *Materials* **2009**, 2, 499-513.
26. Thampi, S. P.; Golestanian, R.; Yeomans, J. M., Vorticity, defects and correlations in active turbulence. *Philos Trans A Math Phys Eng Sci* **2014**, 372.
27. Aditi Simha, R.; Ramaswamy, S., Hydrodynamic fluctuations and instabilities in ordered suspensions of self-propelled particles. *Phys Rev Lett* **2002**, 89, 058101.
28. Voituriez, R.; Joanny, J. F.; Prost, J., Spontaneous flow transition in active polar gels. *Europhysics Letters (EPL)* **2005**, 70, 404-410.